

# Analysis investigation of composite lattice conical shell as satellite carrier adapter for aerospace applications

Research Article

M. FarhadiNia<sup>1</sup>, Nader Namdaran<sup>1,\*</sup>, J. E. Jam<sup>1</sup>, M. Zamani<sup>1</sup>, O. Yaghobizadeh<sup>1</sup>,  
S. M. Gharouni<sup>1</sup>

<sup>1</sup>Composite Materials and Technology Center, MUT, Tehran, Iran

Received 13 March 2014; accepted (in revised version) 27 May 2014

**Abstract:** In this research paper, mechanical behavior of the satellite carrier adapter composed of composite lattice shell is investigated. First, geometric parameters of the composite lattice shell are analyzed. Then, the existing criteria for choosing the fiber path definition for winding of the fibers (i.e. geodesic trajectory) are presented, and the governing mechanical and geometric relations of the structure are derived. Later, stiffness matrix of the structure is obtained, according to the foregoing relations. Finally, utilizing the finite element modeling of a conical lattice shell specimen, a relative comparison is made between the results of the finite element method and the analytical method. Analytical and numerical results obtained, indicate that the axial strain of the structure undergoes a nonlinear reduction with the increase of the thickness and width of the ribs.

**MSC:** 94C30 • 74S05

**Keywords:** Composite structures • Lattice conical shell • Spacecraft carrier adapter • Helical and circumferential ribs • FEM.

© 2014 IJAAMM all rights reserved.

## 1. Introduction

Traditionally, lightweight metals were used as basic materials for aerospace structures, but during the last decades, in many applications, fiber reinforced composites started to appear, promising further substantial weight savings, as well as satisfying higher strength requirements. Due to the different mechanical behavior of these materials, new design and analysis strategies, besides production methods had to be developed, in order to fully exploit their superior properties.

Composite lattice shells have now become a popular choice in many state of the art aerospace applications. They are used in various structural components, such as: rocket interstages, satellite carrier adapters for spacecraft launchers, payload fairings (launch vehicle fairings), radomes, spacecraft fittings, missile motor cases, fuselage and fuel tank components for aerial vehicles, and also parts of deployable space antennas.

The history of the lattice structures development, review of the founding studies, and analysis of design approaches and fabrication techniques are introduced by Vasiliev et al. [1-3].

Tsai et al. [4] did one of the most comprehensive researches on lattice patterns, wherein more detailed analysis of grid structures is included, a method for optimum design is established, and multiple loads and failure mechanism are considered. They investigated the effects of different loadings on lattice patterns and made good comparisons with regard to mechanical properties among lattice, sandwich and laminate structures.

Numerical optimization of annular lattice structures under axial compression is done in reference [5]. In [6] design and optimization of laminated conical shells for buckling and maximum buckling loads has been performed. In

\* Corresponding author.

E-mail address: [nader\\_namdaran@yahoo.com](mailto:nader_namdaran@yahoo.com)

this study, optimization has been exerted in two states of causing the maximum buckling load at certain weight, and causing the minimum weight under a constant critical load.

In [7] critical buckling load is derived from the solution of the governing nonlinear partial differential equation with different coefficients. In [8] buckling of the cylindrical lattice structure has been done, using finite element method. The parametric finite-element buckling analyses of the anisogrid conical shells subjected to axial compression, transverse bending, pure bending, and torsion have been performed.

In [9] buckling analysis of the conical lattice shell is studied, using a numerical code, which determines basic parameters, buckling under critical axial loading, torsion moment, and bending moment. The lattice shell is modeled as a three-dimensional frame structure composed of curvilinear ribs subject to tension/compression, bending in two planes and torsion.

General buckling of the structure, local buckling of helical ribs and failure of helical and hoop ribs are critical cases for the evaluation of strength of the lattice shell. In this research paper, the mechanical behavior of the lattice conical shell (satellite carrier adapter) is investigated under axial compressive loading. Based on this, first of all, the geometric parameters of the lattice conical shell are investigated. Winding of fibers is accomplished according to the application and the type of loading to which the lattice structure is subject, and as a result the geodesic trajectory has been chosen for the design procedure of this structure, then the failure relations for the shell ribs are derived, and finally using a finite element model, the results of the analytical method solution are compared with the FEM results.

## 2. Design and analysis

### 2.1. Geometric Parameters

Grid stiffened structures, or otherwise known as lattice structures are the most advanced and state of the art patterns in the design of composite structures, although they have been traditionally used in classic metal structures from a long time ago. Application of composite structures makes it possible to utilize longitudinal (fiber direction) properties of composite materials in the different desired orientations of the structure. This fact is one of the major characteristics of using these structural elements in structures composed of composite materials. Lattice structures just like other structures possess geometrical variables, which matter in the design and optimization procedures. These variables determine the configuration of the lattice structures, including: angle ( $\phi$ ) thickness ( $H$ ), and the distances between ribs ( $a_c, a_n$ ). A sample prototype of a lattice structure with internal skin and its different parameters is shown in Fig. 1. Besides, lattice structures have different configurations, hence having different properties. Generally these configurations can be investigated from the perspective of three different categories:

1. Properties and mechanical efficiency
2. Type of design and optimization procedure
3. Easiness of production and manufacture

Besides having potential mechanical properties, lattice structures composed of composite materials possess conspicuous characteristics, like being extremely light and bearing huge loads at the same time. Because of these characteristics, lattice structures have been increasingly used in the manufacture of airplane and satellite systems. A prototype of spacecraft carrier adapter separately made of Aluminum and composite materials is shown in Fig. 2. Application of the composite prototype resulted in 30 percent of weight loss, compared to the conventional metallic prototype. Spacecraft carrier adapter has the duty of carrying the satellite and putting it into the orbit of the earth. Utilizing composite lattice shells, as spacecraft carrier adapters, individually or together with other lower and upper shells, has led to a noticeable weight loss and strength increase. A view of the application of spacecraft carrier adapter at the lower section of the satellite system has been portrayed in Fig. 3.

### 2.2. Constraints

Composite shells designed for aerospace applications with regard to the type of their application, have limitations. The curvature of fiber trajectory ( $k$ ) is one of the constraints, which usually plays an important role in the design of lattice structures under axial compressive loads [6]. Regarding this fact, the following relations are derived:

$$\begin{cases} k(x, T) \leq k_{\max} & x \in [0, L] \\ k(x, T) \geq -k_{\max} & x \in [0, L] \end{cases} \quad (1)$$

A view of flattened truncated cone configuration is shown in Fig. 4.

Regarding Eq. (1) and Fig. 1, we have:

- $X$  = Longitudinal distance of the coordinates of points on the shell surface from the smallest radius
- $L$  = Length of the cone along the surface

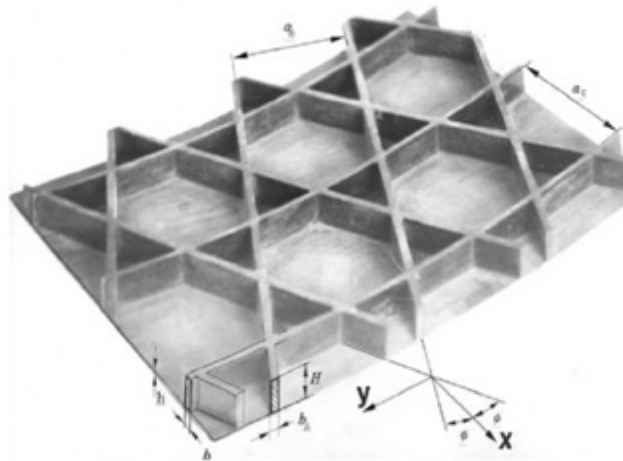
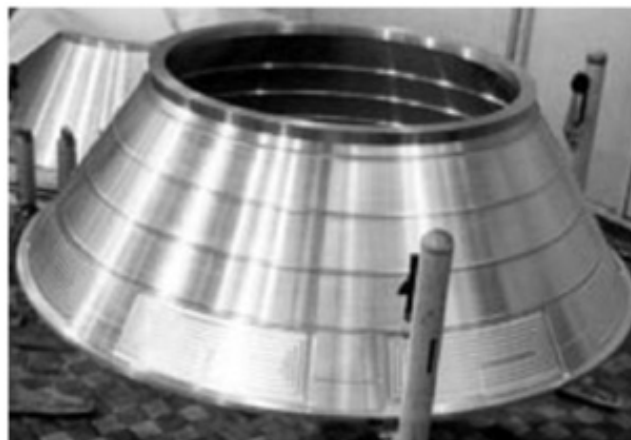
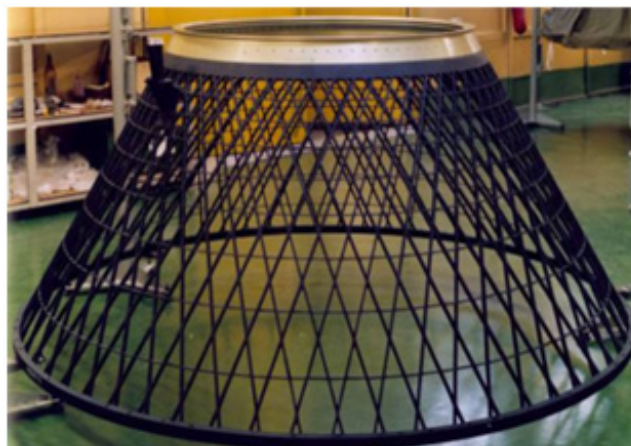


**Fig. 1.** A view of the lattice structure with lower skin [1]



(a)



(b)

**Fig. 2.** Composite lattice shell (spacecraft carrier adapter) composed of: (a) composite, (b) metal materials [1]

$k$  = Curvature of the trajectory

$T$  = Angle of fiber on each distance from the apex of the cone, relative to the line passing through the apex and tangent to the shell

Regarding Fig. 4, the angle between border  $\hat{a}$  (along the length) and tangent to the fiber in each zone is shown with  $\phi$ .

Also, some of the geometric parameters used to derive the equations governing the winding of fibers are shown in Fig. 5.

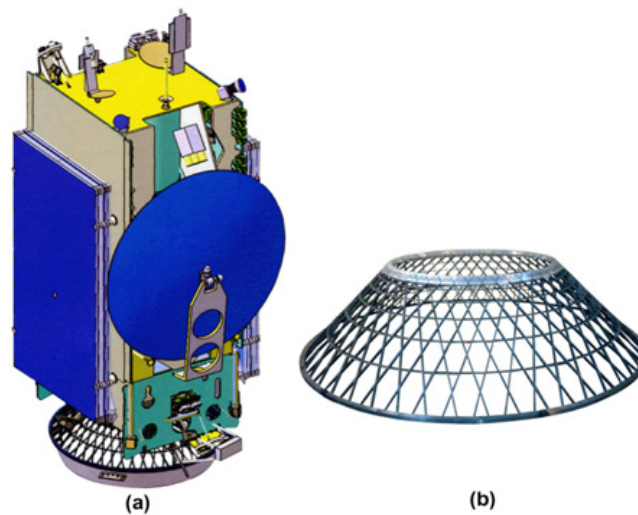


Fig. 3. A view of the application of spacecraft carrier adapter at the lower section of a satellite system [2]

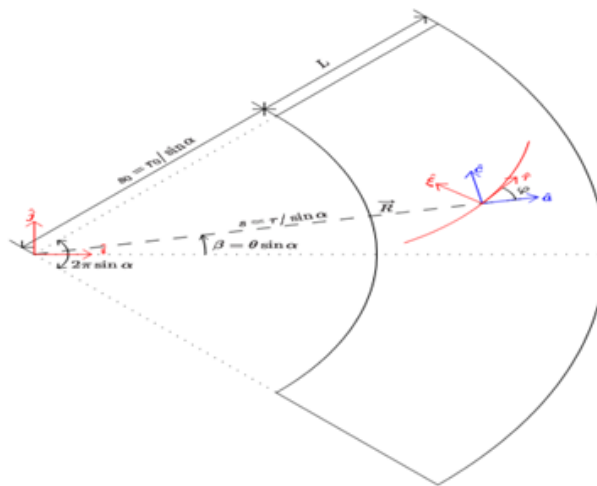


Fig. 4. A flattened truncated cone configuration [6]

Considering Fig. 5, the following parameters are defined:

- $r_o$  = Radius of the cone small cross-section
- $r_1$  = Radius of the cone big cross-section
- $A$  = Axial length of the cone
- $L$  = Length of the tangent to the cone
- $\alpha$  = Angle of edge of the cone relative to the axis of the cone

The angle  $\alpha$  is achieved as:

$$\tan \alpha = \frac{r_1 - r_o}{A}, \quad \sin \alpha = \frac{r_1 - r_o}{L} \quad (2)$$

Since, radius of the cone changes by location, therefore the radius could be expressed as a function of the variable  $x$ .

$$r(x) = r_o + x \sin \alpha \quad (3)$$

The longitudinal coordinate of the surface of the cone  $s(x)$  as the longitudinal distance from the vertex of the cone to any point on its surface is defined as:

$$s = \frac{r(x)}{\sin \alpha} = x + \frac{r_o}{\sin \alpha} \quad (4)$$

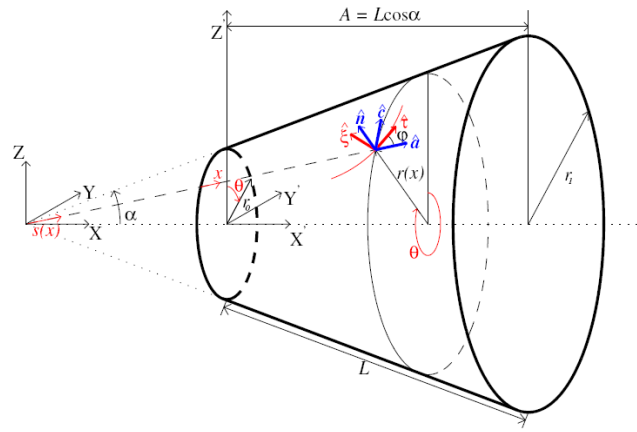


Fig. 5. Geometry of the truncated cone [7]

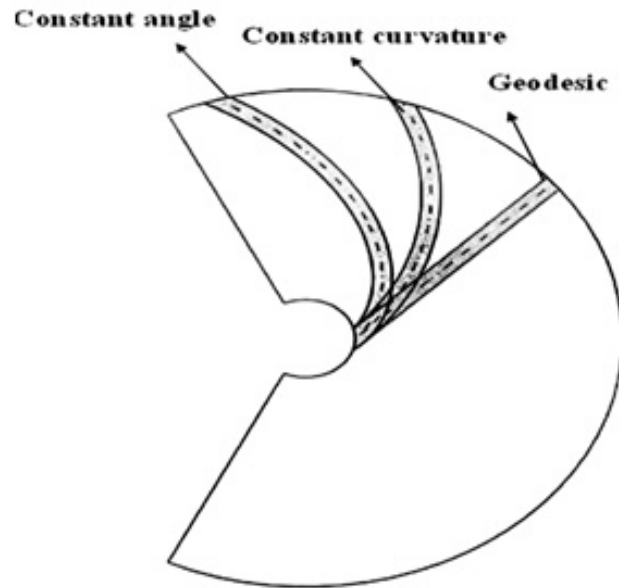


Fig. 6. Three fiber paths on the flattened cone [7]

Considering the above Fig. 5,  $\hat{a}$  and  $\hat{c}$  are unit vectors for the longitudinal and circumferential surface directions of the conical shell, respectively, and  $\hat{n}$  is also the surface normal (perpendicular unit vector to the surface of the cone) used in the fiber path definitions.

$$dx = ds, r(x)d\theta = sd\beta \quad (5)$$

### 2.3. Fiber path trajectories on the shell surface

In order to produce shells of revolution by the filament winding machine, several winding methods are used. The winding process is carried out with regard to the application of the shell and type of loading to which the structure is subject. Fiber placement methods in filament winding consist of three different types, namely: geodesic, constant angle, and constant curvature. As we continue, the conventional fiber laying methods on the mandrel are investigated, and finally the appropriate method is chosen based on the most important parameter (loading). In Fig. 6 an overview of the three fiber trajectories discussed is exhibited.

#### 2.3.1. Geodesic fiber path

This path is named after the name of the shortest possible path. The shortest distance between two points on the surface of any shell of revolution, is called the geodesic path. This is in a way that, if the two points are connected using a string, and the shell is flattened, then the curvature of the path of the string is zero. The following are the

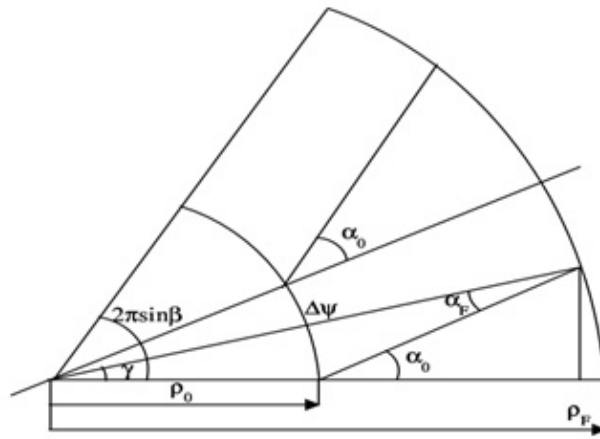


**Fig. 7.** Expanded section of the truncated conical shell

governing equations for the geodesic state [10]:

$$\sin \phi(x) = \frac{r_0 \sin T_0}{r(x)} = \frac{s_0 \sin T_0}{s} \tag{6}$$

where  $T$  is the fiber angle at the small side of the cone, and can vary in between  $-90$  and  $+90$ . As it was stated, the curvature of this path is one of the main constraints and is equal to zero [10].

$$k(x) = 0 \tag{7}$$

### 2.3.2. Constant angle path

In the constant angle state, winding of the fibers is performed with a special rate that a fixed angle takes place all through the path [10].

$$\begin{cases} \phi(x) = \phi \\ \frac{d\theta}{dx} = \frac{\tan \phi}{r(x)} \end{cases} \tag{8}$$

Curvature of the trajectory is calculated as follows:

$$k(x) = \frac{\sin \alpha \sin \phi}{r(x)} \tag{9}$$

### 2.3.3. Constant curvature path

Finally, a path with constant curvature is defined, so that the curvature constraint can be readily evaluated. In this state, the equations are given below, and angle variation is obtained by the following equation [10]:

$$\sin \phi(x) = \frac{r_0 \sin T_0}{r(x)} + \frac{\kappa}{\sin \alpha} \left( \frac{r(x)^2 - r_0^2}{2r(x)} \right) = \frac{s_0 \sin T_0}{s} + \kappa \left( \frac{s^2 - s_0^2}{2s} \right) \tag{10}$$

Having  $T$  as the fiber angle at the small cross-section of the cone, and  $T_1$  as the fiber angle at the bigger cross-section of the cone, curvature of the path length is defined as [10]:

$$\kappa = \left( \frac{r_1}{\bar{r}} \sin T_1 - \frac{r_0}{\bar{r}} \sin T_0 \right) \frac{1}{L}, \quad \bar{r} = \frac{r_0 + r_1}{2} \tag{11}$$

Constant curvature path could be located between two or more circular ribs. According to the discussions above, the first step is to select the best path for winding of fibers. Since the basis for the design of lattice structures is axial compressive loading, the most important problem arising is the issues of buckling and elastic stability of these structures. By these discussions, it is determined that the design of the lattice structure and eventually its manufacture, must be carried out in a state that presents the best possible strength against buckling. By the study of the characteristics of winding of fibers, the geodesic trajectory is known to be the best fiber winding path for the design and analysis of lattice structures in the face of axial compressive loads. Since this fiber path has zero curvature, it has the least sensitivity compared to the other two types of fiber paths. Therefore, taking the above descriptions into consideration, the geodesic fiber trajectory is chosen as the fiber system for the analysis of the conical lattice shell.

## 2.4. Stiffness matrix of the lattice conical shell

Lattice structures are made of a number of helical and circular ribs. The design parameters are determined on the basis of the location of helical and circular ribs. Some of these parameters depend on the angel of helical ribs, and some othersnot only depend on the angle of the cone, but also depend upon the height of the structure, and by the increase of the height, have variations with a certain rate.Because of the complexity of the geometry of conical lattice shells, in order to initiate the design procedure, one must first investigate the effective design parameters of the structure, which are categorized into two groups of dependent and independent parameters [11].

### - Dependent parameters

Dependent parameters include:  $\Delta\psi, \phi, \lambda, a_c,$  and  $a_h$ .

### - Independent parameters

The number of circular and helical ribs ( $n_c, n_h$ ), and thickness of shell, serve as the independent parameters in the design of conical lattice structure.

A schematic of the parameters stated here in the design of conical lattice structure, is shown in Fig. 7. In order to derive the governing equations of the lattice conical shell structure, first some geometric parameters must be defined. In this stage, a section of the cone is developed, and then the equations are derived.By using the geodesic relations of the line passing through the apex of the truncated cone and the cone itself,the geodesic angle at any point on the surface is achieved as [5]:

$$\rho \sin \phi = \rho_o \sin \phi_o = C_o = \text{constant} \quad (12)$$

where,  $\rho = \frac{r}{\sin \alpha}$  and  $r$  is the radius of the cone which is different at any point, and  $\alpha$  is the angle of the line passing through the cone and the axis of the cone. Taking derivation from (1) one has:

$$\frac{d\rho}{\rho} = -\frac{d\phi}{\tan \phi} \quad (13)$$

where  $\Delta\psi$  is the angle between each two helical ribs as indicated in Fig. 7.

$$\Delta\psi = \frac{2\pi \sin \alpha}{n_h} \quad (14)$$

Geometric and finite element designs of lattice conical shell, is performed with this assumption that, the circular ribs are located between the intersections of the helical ribs.

Considering the geometry of Fig. 7, the following equation is achieved:

$$\gamma = \frac{\Delta\psi}{2}(n_c - 1) \quad (15)$$

Now using (12),  $\phi_F$  is expressed as function of  $\phi_o$ . Equation of  $\phi_o$  is computed as follows:

$$\phi_o = \tan^{-1} \left( \frac{\rho_F \sin \gamma}{\rho_F \cos \gamma - \rho_o} \right) \quad (16)$$

Geodesic angle at the bigger cross-section ( $\phi_F$ ) is computed as follows:

$$\phi_F = \phi_o - 1 \quad (17)$$

Variations of  $\rho$  versus  $\phi$  are achieved by this equation:

$$d\rho = -C_o \frac{\cos \phi}{\sin^2 \phi} d\phi \quad (18)$$

Vertical space between circular and helical ribs for a cell at each row is derived according to the following equations:

$$a_h = 2a_c \sin \phi \quad (19)$$

$$(a_c)_{i,i+1} = -\frac{\int_{\rho_i}^{\rho_{i+1}} \Delta\psi d\rho}{\int_{\phi_i}^{\phi_{i+1}} 2d\phi} \quad (20)$$

In (20) ,  $i$  indicates the number of the ribs. The negative sign in (20) means that the axis of the coordinate system is located on the smaller cross-section. Stiffness properties of one representative cell created by a repeated pattern represent the stiffness properties of the overall repeating structural elements. Orthotropic properties regarded for conical shells are along the direction of the axis. To set an example for the cylindrical shell, stiffness along the axial direction is equal to  $\bar{E}_x \frac{A}{L}$ , where  $A = 2\pi RH$  is the cross-section of the structure. Paying attention to Fig. 7, the stiffness matrix of the cells  $[Q]$  can be derive with due regard to the order of the ribs [5]:

$$[Q] = \begin{bmatrix} \frac{2E_h b_h}{a_h c^4} & \frac{2E_h b_h}{a_h s^2 c^2} & 0 \\ \frac{2E_h b_h}{a_h s^2 c^2} & \frac{2E_h b_h}{a_h s^4} + \frac{E_c b_c}{a_c} & 0 \\ 0 & 0 & \frac{2E_h b_h}{a_h s^2 c^2} \end{bmatrix}, \quad s = \sin \phi, \quad c = \cos \phi \tag{21}$$

The moduli of elasticity of the helical and circular ribs are  $E_h$  , and  $E_c$  , respectively. Equation (21) is derived from the theories and formulations associated with the stiffness of the layer and fiber properties. Properties of the equal stiffness along the axial direction are derived from the relation below [5]:

$$\bar{E}_x = \frac{1}{H} \left( \frac{q_{11}q_{22} - q_{12}^2}{q_{22}} \right) \tag{22}$$

The  $q_{ij}$  used in eqref22 are components of the stiffness matrix  $[Q]$ . As it is seen,  $\bar{E}_x$  depends upon the angle of helical ribs, width of ribs, and distance between helical and circular ribs.

### 2.5. Stress strain relations in a conical lattice shell

In order to investigate the yielding of the ribs in the lattice conical shell, the stress strain relations are used. Considering the above-mentioned facts, the stress strain relations of the ribs are similar to isotropic materials, and conform to Hooke's law,  $\sigma = E \varepsilon$ , and govern both local and global stresses and strains [5]:

$$\varepsilon = \varepsilon_x \cos^2 \phi + \varepsilon_h \sin^2 \phi + \gamma_{xh} \sin \phi \cos \phi \tag{23}$$

From the above relation,  $\varepsilon_x$  and  $\varepsilon_h$  are strains in the rib and circumferential directions, respectively, and also  $\gamma_{xh}$  is the shear strain. General stress in the rib direction is calculated using the two helical ribs, constricting the angle ( $\pm\phi$ ) with respect to each other.

$$\begin{cases} \sigma_x = \sigma_x V_{f\phi} \cos^2 \phi + \sigma_{-x} V_{f-\phi} \cos^2 \phi \\ \sigma_x = (\varepsilon_x \cos^2 \phi + \varepsilon_h \sin^2 \phi) 2E_h V_{f\phi} \cos^2 \phi \end{cases} \tag{24}$$

$V_{f\phi}$  and  $V_{fh}$  are derived from (25):

$$\begin{cases} V_{f\phi} = V_{f-\phi} = \frac{b_h}{a_h} \\ V_{fh} = V_{f-h} = \frac{b_c}{a_c} \end{cases} \tag{25}$$

For calculation of the general stress along the circumferential direction ( $\sigma_h$ ), we have three effective parameters, two of which depend upon the helical ribs:

$$\begin{cases} \sigma_h = \sigma_\phi V_{f\phi} \sin^2 \phi + \sigma_{-\phi} V_{f-\phi} \sin^2 \phi + \sigma_h V_{f\phi} \\ \sigma_h = (\varepsilon_x \cos^2 \phi + \varepsilon_h \sin^2 \phi) 2E_h V_{f\phi} \cos^2 \phi + \varepsilon_h E_c V_{f\phi} \end{cases} \tag{26}$$

Accordingly, the shear stress is also becomes:

$$\sigma_h = (2E_h V_{f\phi} \cos^2 \phi \sin^2 \phi) \gamma_{xh} \tag{27}$$

## 3. Results and discussion

### 3.1. Investigation of geometric variations of the lattice conical shell

In order to design the fiber path for the helical and hoop ribs of the lattice conical shell, it is necessary to derive the geodesic angles of the helical ribs at the big and small cross-sections, and also the height position of the lattice shell. From (16), (17) and (20), so as to design the lattice conical shell, general dimensions, including: height, bigger cross-section, smaller cross-section, as well as the apex angle of the cone must be determined. The diameters of the bigger and small cross-sections are: 2500 mm, and 1250 mm, respectively, and the apex angle is supposed to be: 34.7 degrees. Now, considering the geometric specifications of the cone, variations of the geodesic angle at its different height locations of the cone, and the number of hoop ribs are specified. With regard to the previous relations stated above, variations of the geodesic angle at the bigger and smaller cross-sections, versus the increase of the height of the cone and increase of the number of the hoop ribs, have been shown in Fig. 8 and Fig. 9, respectively. As it is noticed, with the increase of the height of the cone, geodesic angles undergo changes and decrease non-linearly. Also, with the increase of the number of the number of hoop ribs under equal geometric conditions, geodesic angles decrease at each cross-section. Results indicate that with the increase of the number of hoop ribs, variations of the geodesic angle at the bigger cross-section have more inclination in their decrease with respect to the smaller cross-section.



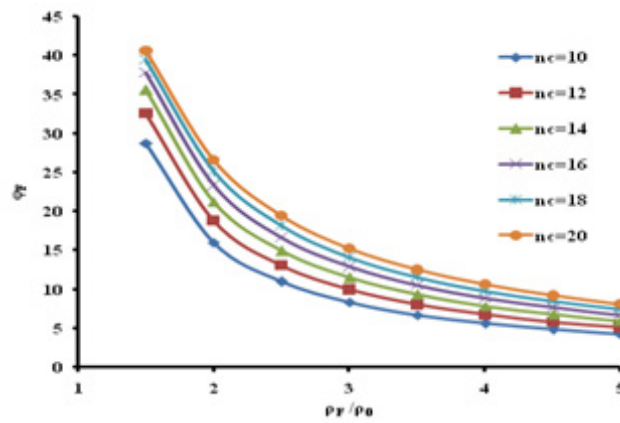


Fig. 8. Variations of  $\phi_F$  versus  $\frac{\rho_F}{\rho_0}$

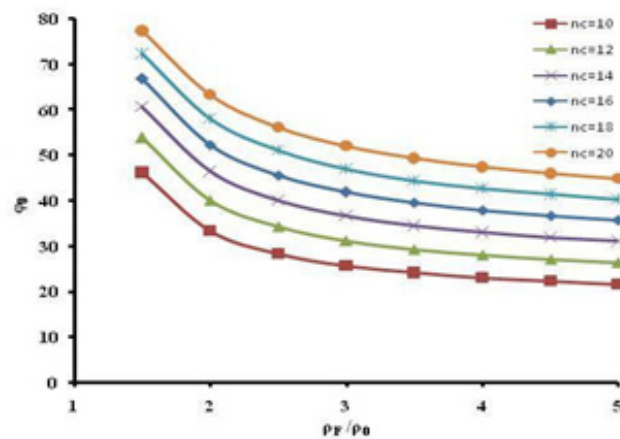


Fig. 9. Variations of  $\phi_0$  versus  $\frac{\rho_F}{\rho_0}$

### 3.2. Finite element model

With due regard to the dependent and independent parameters of the geometry of the lattice conical shell, the design of its finite element model is presented. Noticing the total geometry of the lattice conical shell, from Fig. 8 and Fig. 9, the geodesic angle is determined at any height location. One can perform the design of the lattice conical shell by finding these angles. The finite element model created is a wire model, and Timoshenko's beam element, has been used for meshing the structure, as in Fig. 10. The use of the beam element for the analysis of the lattice conical shell is assessed in [1]. Also, from the point of view of the geometric specifications of the lattice conical shell, this type of element (beam type) is evaluated as the most proper element for performing the analysis, as in Fig. 11.

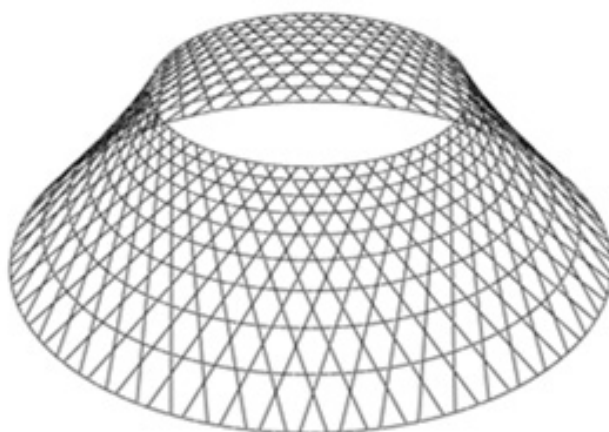
Geometric specifications of the lattice conical shell are summarized in Table 1. Also, properties of the materials used in the lattice conical shell are included in Table 2.

### 3.3. Comparison of analytical results and numerical results for the investigation of the behavior of lattice conical shell

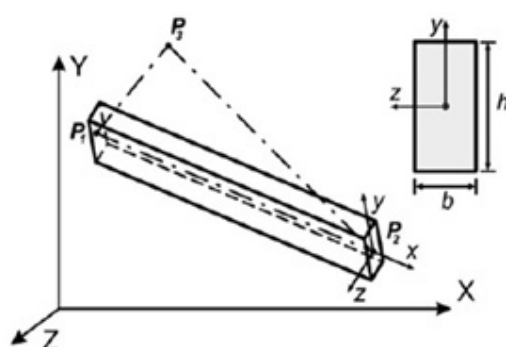
For the finding the distribution of stress and strain in the lattice conical shell under compressive axial loading, the stiffness matrix of the shell has to be found first. The stiffness matrix in circumferential, axial, and tangent to the surface directions is achievable according to Eqs. (20) and (21). Following this procedure, distribution of stress and strain in different sections of the lattice conical shell in the three stated directions is investigated. By deriving the

Table 1. Geometric parameters of the lattice conical shell studied

$n_c$	$n_h$	$\alpha_f$	$\alpha_0$	$H$ (mm)	$b_c$ (mm)	$b_h$ (mm)
5.75	4	18	33.44	15.98	53	10



**Fig. 10.** Finite element model of the lattice conical shell, made by ABAQUS software



**Fig. 11.** A schematic of the beam element used in finite element analysis

equivalent stiffness matrix, one can achieve the strain of the structure with regard to the distribution of axial compression. A compressive load equal to 1 megaNewton is applied to the small cross-section. Afterwards, investigation of the average variations of the axial strain of the lattice conical shell is carried out by means of the finite element analysis with due regard to the variations of the width and thickness of ribs.

**3.3.1. Strain distribution in helical ribs versus width variations of the shell using analytical and numerical methods**

Distribution of strain using analytical and numerical methods for the lattice conical shell is shown in Fig. 12. Results indicate that by the increase of the thickness of helical and circumferential ribs, the strain induced in the lattice conical shell decreases non-linearly. Also, with the increase of the thickness, the discrepancy between analytical and numerical results increases and this increase indicates the decrease of the accuracy of the beam element in the implementation of the finite element analysis. For this shortcoming, one must use other types of element like the three dimensional solid element. A schematic of the finite element analysis of the lattice conical shell with the dimensions (thickness of 18 mm and width of 5.75 mm) is presented in Fig. 13.

**3.3.2. Strain distribution in helical ribs versus thickness variations of the shell using analytical and numerical methods**

Fig. 4 demonstrates a view of strain variations of the lattice conical shell in the axial direction versus variations of the thickness of circumferential and helical ribs. Results indicate that the strain induced in the lattice conical shell decreases non-linearly with the increase of the thickness of the circumferential and helical ribs.

**Table 2.** Properties of the materials used in the lattice conical shell

$E_h$ (GPa)	$\bar{\sigma}_h$ (MPa)	$m_h$ (Kg/m <sup>3</sup> )	$E_c$ (GPa)	$m_c$ (Kg/m <sup>3</sup> )
1410	64	1450	350	80

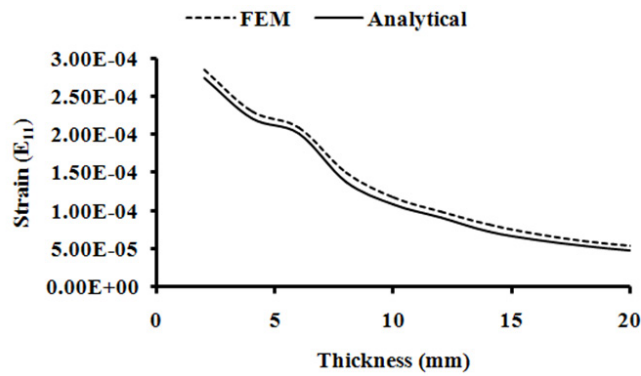


Fig. 12. Comparison of analytical and finite element methods for the strain induced in the lattice conical shell under axial compression with variation of the thickness of ribs

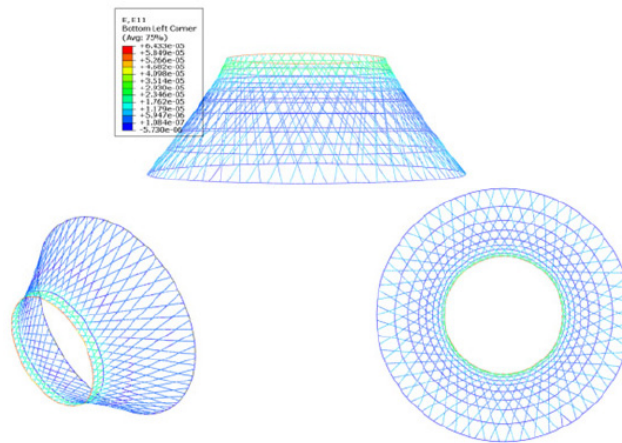


Fig. 13. A plot of the strain of the lattice conical shell in the axial direction

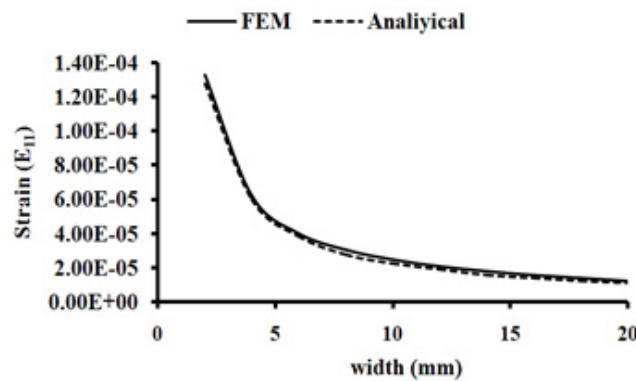


Fig. 14. Comparison of analytical and finite element methods for the strain induced in the lattice conical shell under axial compression with variations of the width of ribs

## 4. Conclusion

In order to design the lattice conical shell, the best fiber path trajectory for winding of fibers has to be chosen. Geodesic trajectory is known to be the best fiber path for increasing the strength of the lattice conical shell structures in the face of axial compressive loads. Therefore, all the equations are derived on the basis of the geodesic fiber path. The distance between circular ribs plays the most important role in the design of the lattice conical shell. This parameter also depends upon the geodesic angles at different height sections of the cone. Comparison of the analytical and finite element analyses of the axial strain variations for the lattice conical shell, versus increase of the thickness and width under compressive loads, indicates that the analytical method according to the derived equations for evaluation of the strain of the lattice conical shell, are of high accuracy. In addition to this, with the

increase of the thickness and width of the helical and circular ribs, the strain induced in the lattice conical shell structure is reduced. Also, analytical results indicate that with the increase of the thickness and width of the circular and helical ribs, other elements like the three dimensional solid and shell elements have to be used.

## References

---

- [1] V. V. Vasiliev, V. A. Barynin, A. F. Razin, Anisogrid lattice structures—survey of development and application, *Compos Struct.* 54 (2001) 361-370.
- [2] V. V. Vasiliev, A. F. Razin, Anisogrid composite lattice structures for spacecraft and aircraft applications, *Compos Struct.* 76 (2006) 182-189.
- [3] V. V. Vasiliev, V. A. Barynin, A. F. Rasin, S. A. Petrokovskii, V. I. Khalimanovich, Anisogrid composite lattice structures-development and space applications, *Compos Nanostruct.* 3 (2009) 38-50.
- [4] S. W. Tsai, H. J. Chen, Analysis and optimum design of composite grid structures, *Composite Materials journal* 30 (1996) 503-534.
- [5] G. Totaro, Z. GÅijrdal, Optimal design of composite lattice shell structures for aerospace applications, *Aerospace Science and Technology* 13 (2009) 157-164.
- [6] Y. Goldfeld, J. Arbocz, A. Rothwell, Design and optimization of laminated conical shells for buckling, *Thin Walled Structures* 43 (2005) 107-133.
- [7] Y. Goldfeld, J. Arbocz, Buckling of laminated conical shells taking into account the variations of the stiffness coefficients, *AIAA J.* 42(3) (2004) 642-649.
- [8] E. V. Morozov, A. V. Lopatin, V. A. Nesterov, Finite-element modelling and buckling analysis of anisogrid composite lattice cylindrical shells, *Compos Struct.* 93 (2011) 308-323.
- [9] E. V. Morozov, A. V. Lopatin, V. A. Nesterov. Buckling analysis of anisogrid composite lattice conical shells, *Composite Structures* 93 (2011) 3150-3162.
- [10] C. M. Poulsen, "Geodetic construction. Part 1", How the Vickers—Armstrong Wellington is built: solving novel and sometimes difficult production problems. *Aircraft Production* (1940) 143-148.
- [11] V. A. Bunakov, Design of axially compressed composite cylindrical shells with lattice stiffeners, in V. V. Vasiliev, Z. GÅijrdal (Eds.), *Optimal Design-Theory and Applications to Materials and Structures*, Technomic Publishing Co. Inc., Lancaster, Basel, 1999.